SIMULATION OF RESERVOIR BEHAVIOUR OF THE GEOTHERMAL FIELDS: HAMAR, N-ICELAND AND PODHALE, S-POLAND

Piotr Dlugosz,
UNU Geothermal Training Programme,
Orkustofnun - National Energy Authority,
Grensasvegur 9,
108 Reykjavik,
ICELAND

Permanent address:
Polish Academy of Sciences,
Minerals and Energy Economy Research Centre,
Jozefa Wybickiego 7,
31-261 Krakow,
POLAND

ABSTRACT

The calibration of geothermal reservoir parameters and future predictions of its behaviour, based on a distributed parameter model, are the main parts of this report. In the first part, the Hamar geothermal field in N-Iceland is considered where measured and calculated water heads, silica concentration and reservoir temperature are fitted together. The monthly production from 1970 to 1991 is used in the calibration. After calibration, the future prediction of the reservoir behaviour was made, with different production rates, until the year 2006. A constant lowering of the water level is observed but with a tendency towards a semi-steady state if the production rate does not exceed 40 l/s. In the case of a constant pumping rate of 40 l/s, one can expect the drawdown in the year 2006 to be approximately 62 m. Future predictions of reservoir temperature indicate almost no changes within the next 15 years. The second part consists of the calculation of drawdown and temperature within a geothermal doublet, located in Podhale geothermal field, S-Poland, with production-injection rates of 20 l/s, 50 l/s and 100 l/s. The initial temperature of the production well is 86°C and after extraction of heat, in a heat exchanger, the water is cooled down to 30°C before it is injected back into the reservoir. The distance between the production well and the reinjection well is about 1200 m. The practical lifetime of a geothermal doublet, for a prescribed temperature drop of 3°C and for the above mentioned production-injection rates are respectively 220, 84 and 44 years of exploitation.

TABLE OF CONTENTS

LIST OF FIGURES

LIST OF TABLES

1. INTRODUCTION

Poland is relatively rich in low enthalpy geothermal resources. They are located in the sedimentary basins of the Polish Lowland. The sedimentary subbasin in Podhale Region is an example of these geothermal resources. To be able to correctly utilize the geothermal energy, effective use of geothermal reservoir engineering methods is necessary in order to provide the appropriate answers to questions on future reservoir behaviour.

The author had the opportunity to become acquainted with reservoir engineering methods during his six month's training at the UNU Geothermal Training Programme at the National Energy Authority in Reykjavik, Iceland in 1991. The programme started with an introductory course related to all aspects of geothermal utilization. Afterwards the author received specialized lectures and took part in practical exercises in borehole geophysics and reservoir engineering. To become acquainted with the state of development in the Icelandic geothermal sector, a field excursion and seminars were organized. The last part of the training concentrated on theoretical studies and practical applications of modelling of Icelandic and Polish geothermal fields.

2. THEORY AND MATHEMATICAL BACKGROUND

2.1 Equations governing reservoir behaviour

The basic equation describing three-dimensional flow in a porous media, can be derived by the use of the mass conservation law and control volume approach.

Referring to Figure 1, the difference in mass flux across two planes normal to the x-axis may be expressed as:

Outflow rate − Inflow rate =

$$(\rho Q)_{\Delta x} - (\rho Q)_{Ox} \qquad (1)$$

where ρ is the density and Q is the volumetric flowrate. A similar expression can be written for the y and z directions. By the assumption that the dimensions of the control volume are very small, the outflow terms can be expressed in a Taylor series as follows:

FIGURE 1: Control volume for mass balance calculation

$$(\rho Q)_{\Delta x} = (\rho Q)_{Ox} + \frac{\delta}{\delta x}(\rho Q)\Delta x + O(\Delta x^2) \qquad (2)$$

For small Δx, the last term is negligible and Equation 1 can be written as:

$$Outflow\ rate - Inflow\ rate = \frac{\delta}{\delta x}(\rho Q)\Delta x \qquad (3)$$

The flowrate Q can be expressed as a product of the Darcy velocity and the area normal to the flow:

$$Q_x = q_x \Delta y \Delta z, \quad Q_y = q_y \Delta x \Delta z, \quad Q_z = q_y \Delta x \Delta y \qquad (4)$$

Considering all planes on the control volume, the total difference between inflow and outflow can be expressed as:

$$Outflow\ rate - Inflow\ rate = [\frac{\delta}{\delta x}(\rho q_x) + \frac{\delta}{\delta y}(\rho q_y) + \frac{\delta}{\delta z}(\rho q_z)]\Delta x \Delta y \Delta z \qquad (5)$$

The net rate of mass outflow must be equal to the rate of changes of mass M with time, within the control box, hence:

$$[\frac{\delta}{\delta x}(\rho q_x) + \frac{\delta}{\delta y}(\rho q_y) + \frac{\delta}{\delta z}(\rho q_z)]\Delta x \Delta y \Delta z = -\frac{\delta M}{\delta t} \qquad (6)$$

Let us now consider the amount of water released from a control volume of a confined aquifer. The mass of water in the saturated volume is:

$$M = \rho \varphi \, \Delta x \Delta y \Delta z \tag{7}$$

The change of mass is given by:

$$dM = [\rho \, d(\varphi \Delta z) + \varphi \, \Delta z d\rho] \Delta x \Delta y \tag{8}$$

assuming deformations to be in the z dimension only. Now one can distinguish the following two components of the mass change. The expression:

$$dM_1 = \rho \, d(\varphi \, \Delta z) \tag{9}$$

is the contribution per unit area due to change in pore volume at constant ρ. Thus,

$$dM_2 = \varphi \, \Delta z d\rho \tag{10}$$

is the contribution due to change in water density at constant pore volume. The first component can be expressed by the use of the pore-volume compressibility α_p, defined as:

$$\alpha_p = -\frac{1}{\varphi \, \Delta z} \frac{d(\varphi \, \Delta z)}{d\sigma_z} = \frac{1}{\varphi \, \Delta z} \frac{d(\varphi \, \Delta z)}{dp} \tag{11}$$

from which

$$dM_1 = \rho \, \alpha_p \varphi \, \Delta z dp \tag{12}$$

The second component of mass change can be derived using the definition of the compressibility of water β:

$$\beta = -\frac{1}{V_w} \frac{dV_w}{dp} \tag{13}$$

where, V_w is the volume of water. Assuming that the mass is constant, the definition of density yields:

$$d\rho = -\rho \frac{dV_w}{V_w} = \rho \beta \, dp \tag{14}$$

Hence, the change of mass due to water compressibility becomes:

$$dM_2 = \varphi \, \Delta z \beta \rho \, dp \tag{15}$$

Finally, the total change of mass is:

$$\frac{dM}{\Delta x \Delta y \Delta z} = \varphi \rho (\alpha_p + \beta) dp \tag{16}$$

Equation 16 can also be expressed as a change in volume and

$$\frac{dV_w}{\Delta x \Delta y \Delta z} = \varphi(\alpha_p + \beta)dp \tag{17}$$

At last, taking into account that

$$dp = \rho g \, dh \tag{18}$$

one can define the specific storage as:

$$S_s = \frac{1}{\Delta x \Delta y \Delta z}\frac{dV_w}{dh} = \rho g \varphi(\alpha_p + \beta) \tag{19}$$

S_s is the volume of water released from storage per unit volume of aquifer per unit decline in pressure head and has dimension L^{-1} (McWhorter and Sunada, 1977).

For a confined aquifer, a second specific parameter can be defined, called the storage coefficient:

$$S = S_s b \tag{20}$$

where b is the aquifer thickness.

Coming back to Equation 6 and using Darcy's equation and the specific storage definition, the mass balance can be written as:

$$\frac{\delta}{\delta x}(K_x \frac{\delta h}{\delta x}) + \frac{\delta}{\delta y}(K_y \frac{\delta h}{\delta y}) + \frac{\delta}{\delta z}(K_z \frac{\delta h}{\delta z}) = S_s \frac{\delta h}{\delta t} \tag{21}$$

If we assume the aquifer to be of constant thickness and the flow to be horizontal, Equation 21 becomes:

$$\frac{\delta}{\delta x}(T_x \frac{\delta h}{\delta x}) + \frac{\delta}{\delta y}(T_y \frac{\delta h}{\delta y}) = S \frac{\delta h}{\delta t} \tag{22}$$

where transmissivity is defined as:

$$T = bK \tag{23}$$

Aquifers can lose or gain water through leakage from an upper aquifer. A confined aquifer, which has at least one semipermeable layer, is called a leaky confined aquifer. Figure 2 shows a situation when there is vertical leakage from an upper water table aquifer to a lower main confined aquifer. We assume that the flow in the main aquifer is essentially horizontal, and leakage in the semipermeable strata is essentially vertical.

By defining

$\gamma = k/m(h_o\text{-}h)$ as a vertical leakage rate through the top of a semipermeable layer,
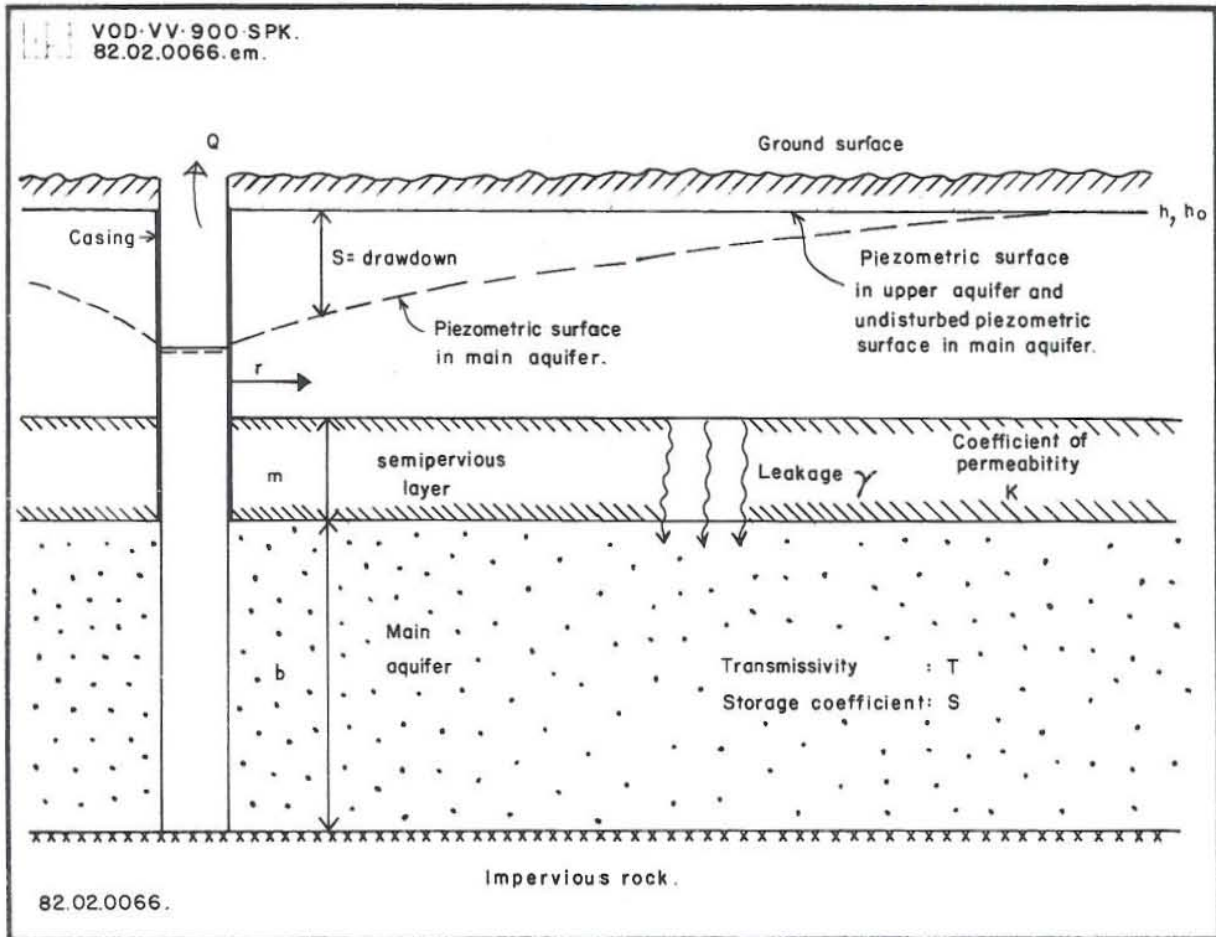
FIGURE 2:   Schematic picture of a leaky confined aquifer

where

h_o - is the head in the upper aquifer above the semipermeable layer,
h - is the head in the main confined aquifer,
k - is the permeability in the semipermeable layer,
m - is the thickness of the semipermeable layer,

the flow balance can be expressed by the following equation:

$$\frac{\delta}{\delta x}(T_x\frac{\delta h}{\delta x}) + \frac{\delta}{\delta y}(T_y\frac{\delta h}{\delta y}) + \gamma = S\frac{\delta h}{\delta t} \tag{24}$$

Equation 24 is the basic continuity equation describing groundwater flow in a leaky confined aquifer, in the absence of sources and/or sinks. In the presence of source with yield Q, Equation 24 becomes:

$$\frac{\delta}{\delta x}(T_x\frac{\delta h}{\delta x}) + \frac{\delta}{\delta y}(T_y\frac{\delta h}{\delta y}) + \gamma + Q = S\frac{\delta h}{\delta t} \tag{25}$$

We remember that in unsteady flow with a declining water table, the dewatering of the pores is not instantaneous, but lags behind the drawdown. From these one can note that S increases at a diminishing rate for the duration of pumping. Boulton (1963) made an assumption concerning the leakage flux caused by drawdown s. He assumed that an increase in drawdown at time t gives rise to a leakage flux, which decreases exponentially with time. Let us consider the mass conservation Equation 24, taking into account changes in storage by water expansion and aquifer compaction and desaturation or drainage of the pores, in polar coordinates:

$$T\left(\frac{\delta^2 s}{\delta r^2} + \frac{1}{r}\frac{\delta s}{\delta r}\right) = S\frac{\delta s}{\delta t} + n\frac{\delta s_o}{\delta t} \tag{26}$$

where

T - is the average transmissivity,

s - is the drawdown as indicated by the difference in the initial, static water level and the water level in a fully penetrating observation well that reflects the average piezometric head over the saturated thickness,

s_o - is the drawdown of the water table,

n - is the effective porosity.

The approximate average value of the Darcy velocity in the vertical direction is:

$$q_z = -K_z \frac{s - s_o}{b_a} \tag{27}$$

where

b_a - is the vertical distance between the water table and the point at which the average drawdown is measured.

Taking into consideration the velocity of the declining water table, one can write:

$$q_z = -n\frac{\delta s_o}{\delta t} \tag{28}$$

Combining (27) and (28), one can receive a linear, first order, nonhomogenous differential equation:

$$\frac{\delta s_o}{\delta t} + \alpha s_o = \alpha s \tag{29}$$

where $\alpha = K_z/nb_a$, and initial conditions are: $s = s_o = 0$ for $t = 0$.

We can solve Equation 29 in the following way. Let us multiply both sides of Equation 29 by $e^{\alpha t}$:

$$\frac{\delta s_o}{\delta t}e^{\alpha t} + \alpha s_o e^{\alpha t} = \alpha s e^{\alpha t} \tag{30}$$

The left hand side of Equation 30 is the derivative of the expression $s_o e^{\alpha t}$. By integrating, we obtain:

$$s_o e^{\alpha t} = \int_0^t \alpha s e^{\alpha \tau} d\tau \tag{31}$$

As a next step, to solve Equation 31 we can use the formula for integration by parts, which finally gives:

$$s - s_o = \int_0^t \frac{\delta s}{\delta t} e^{-\alpha(t-\tau)} d\tau \tag{32}$$

Putting the expression (32) into (26), the differential equation governing the flow in a leaky confined aquifer with delayed yield from storage is obtained:

$$\frac{\delta^2 s}{\delta r^2} + \frac{1}{r} \frac{\delta s}{\delta r} = \frac{S}{T} \frac{\delta s}{\delta t} + \alpha \frac{n}{T} \int_0^t \frac{\delta s}{\delta t} e^{-\alpha(t-\tau)} d\tau \tag{33}$$

2.2   Brief overview of the reservoir modelling methods

Aquifer models can be classified in several ways. We can distinguish between continuous models, and those with a discrete distribution of parameters. The simplest type of a geothermal reservoir model is the lumped parameter model. In this case only the lumped mass within the system and what crosses the boundaries is taking into account. In these models, time is the only independent variable, and the system can, therefore, be described mathematically by the use of ordinary differential equations and, as a result, analytical solutions for the average reservoir parameter can be obtained. Models with distributed parameters, i.e. where the properties of fluid and rock can vary in space, demand larger computers. Models with distributed parameters are often too complex to be treated analytically. In these cases a numerical approach is used (Bodvarsson and Witherspoon, 1989).

At present, with high-speed computers widely available, numerical models are being used extensively for geothermal reservoirs. We can consider, in principle, two types of models: finite difference models and finite elements models. The concept of elements (the subareas delineated by the lines connecting nodal points) is fundamental to the development of equations in the finite element method. Mainly triangular elements are used, but quadrilateral or other elements are also possible. In the difference method, nodes may be located inside cells, or at the intersection of grid lines. The object of modelling is to predict the value of unknown variables (for example groundwater head or concentration of a contaminant) at nodal points. Models are often used to predict the effect of pumping on groundwater levels. However, before a predictive simulation can be made, the model should be calibrated and verified. The process of calibration and verification of the model is the content of the following chapters of this report.

2.3   The main features of the AQUA program

AQUA is a program package developed by Vatnaskil Consulting Engineers (1991) to solve the groundwater flow and transport equations using the Galerkin finite element method. The basis for the mathematical model is the following differential equation:

$$a\frac{\delta u}{\delta t} + b_i\frac{\delta u}{\delta x_i} + \frac{\delta}{\delta x_i}(e_{ij}\frac{\delta u}{\delta x_j}) + fu + g = 0 \tag{34}$$

The model is two-dimensional, and the indices i and j indicate the x and y coordinate axes.

2.3.1 Flow model

For the transient groundwater flow, Equation 34 is reduced to:

$$a\frac{\delta u}{\delta t} + \frac{\delta}{\delta x_i}(e_{ij}\frac{\delta u}{\delta x_j}) + fu + g = 0 \tag{35}$$

For confined groundwater flow, the parameters in Equation 35 are defined as

$$u = h, \quad e_{ij} = T_{ij}, \quad f = 0, \quad g = Q + (k/m)\,h_o \quad \text{and} \quad a = -S - \alpha n\int_0^t \delta/\delta t\, e^{-\alpha(t-\tau)}\,d\tau$$

Equation 35 then becomes:

$$\frac{\delta}{\delta x}(T_{xx}\frac{\delta h}{\delta x}) + \frac{\delta}{\delta y}(T_{yy}\frac{\delta h}{\delta y}) + \frac{k}{m}(h_o - h) + Q = S\frac{\delta h}{\delta t} + \alpha n\int_0^t \frac{\delta h}{\delta t}e^{-\alpha(t-\tau)}d\tau \tag{36}$$

This is the same equation as derived in Chapter 2.1.

To obtain an expression for the numerical solution of Equation 36, the following way is used, step n:

$$i_n = \alpha n\int_0^{t_n} \frac{\delta h}{\delta t}e^{-\alpha(t-\tau)}d\tau \tag{37}$$

and step $n + 1$:

$$i_{n+1} = \alpha n\int_0^{t_{n+1}} \frac{\delta h}{\delta t}e^{-\alpha(t_{n+1}-\tau)}d\tau \tag{38}$$

The integral can be rewritten as:

$$i_{n+1} = e^{-\alpha\Delta t}i_n + \alpha n e^{-\alpha(t_n+\Delta t)}[\frac{1}{\alpha}e^{\alpha\tau}]_{t_n}^{t_{n+1}}\frac{(h_{n+1}-h_n)}{\Delta t} \tag{39}$$

Finally:

$$i_{n+1} = e^{-\alpha\Delta t}i_n + \frac{n}{\Delta t}(h_{n+1}-h_n)(1-e^{-\alpha\Delta t}) \tag{40}$$

Now Equation 36 can be approximated by the following numerical expression:

$$-K[\theta h_{n+1}+(1-\theta)h_n] = \frac{1}{\Delta t}M(h_{n+1}-h_n)+L[\theta i_{n+1}+(1-\theta)i_n] \tag{41}$$

where θ is equal to 1, as the classic implicit approximation.

In AQUA, the following boundary conditions are used:

1. Dirichlet boundary conditions
2. Von Neumann boundary conditions
3. Cauchy boundary conditions

In the Dirichlet boundary conditions the groundwater level, the piezometric head or the potential function is prescribed at the boundary. In the Von Neumann boundary conditions the flow at the boundary is prescribed. The Cauchy boundary condition is a head-dependent condition, where the flowrate is related to both the normal derivative and the head.

2.3.2 Mass transport

The AQUA program can solve the transient transport of mass in which case the parameters of Equation 34 are defined as follows:

$$u = c, \quad a = \varphi b R_b, \quad b_i = V_i b, \quad e_{ij} = -\varphi b D_{ij}, \quad f = \varphi b R_d \lambda + \gamma + Q \quad \text{and} \quad g = -\gamma c_o - Q c_w,$$

where the dispersion coefficients D_{xx} and D_{yy}, are defined as:

$$\varphi D_{xx} = a_L V^n + D_m \varphi \quad \text{and} \quad \varphi D_{yy} = a_T V^n + D_m \varphi.$$

The retardation coefficient R_d is given by:

$$R_d = 1 + \beta(1-\varphi)\rho_s/\varphi\rho_l \quad \text{and} \quad \beta = K_d \rho_l,$$

where

a_L	- is the longitudinal dispersivity (m),
a_T	- is the transversal dispersivity (m),
c	- is the solute concentration (kg/m^3),
c_o	- is the concentration of vertical inflow (kg/m^3),
c_w	- is the concentration of injected water (kg/m^3),
K_d	- is the distribution coefficient,
D_m	- is the molecular diffusivity (m^2/s),
φ	- is the porosity,
V	- is the velocity taken from the solution of the flow problem (m/s),
λ	- is the exponential decay constant (s^{-1}),
γ	- is the vertical leakage rate,
ρ_l	- is the density of the liquid (kg/m^3),
ρ_s	- is the density of the porous medium (kg/m^3).

2.3.3 Heat transport

In a similar way, AQUA is able to handle a single phase heat transport by the use of the following parameters:

$$u = T, \quad a = \varphi b R_h, \quad b_i = V_i b, \quad e_{ij} = -b K_{ij}, \quad f = V + Q, \quad g = -\gamma T_o - Q T_w.$$

The heat dispersion coefficients are given by:

$$K_{xx} = a_L V^n + D_h \varphi \quad \text{and} \quad K_{yy} = a_T V^n + D_h \varphi.$$

The heat retardation coefficient R_h is given by:

$$R_h = 1 + \beta(1-\varphi)\rho_s / \varphi \rho_l,$$

where

T - is the temperature (°C),
T_0 - is the temperature of vertical inflow (°C),
c_l - is the specific heat capacity of the liquid (kJ/kg°C),
c_s - is the specific heat capacity of the porous medium (kJ/kg°C),
D_h - is the heat diffusivity (m²/s).

3. MODELLING OF THE HAMAR GEOTHERMAL FIELD, N-ICELAND

3.1 The main features of the Hamar geothermal field

3.1.1 Locality

The Hamar geothermal field is located in Northern Iceland, about 4 km from the town Dalvik, with a population of 1400 inhabitants. The reservoir has been utilized for district heating since late 1969. The elevation of the field is about 60 m above sea level (Figure 3).
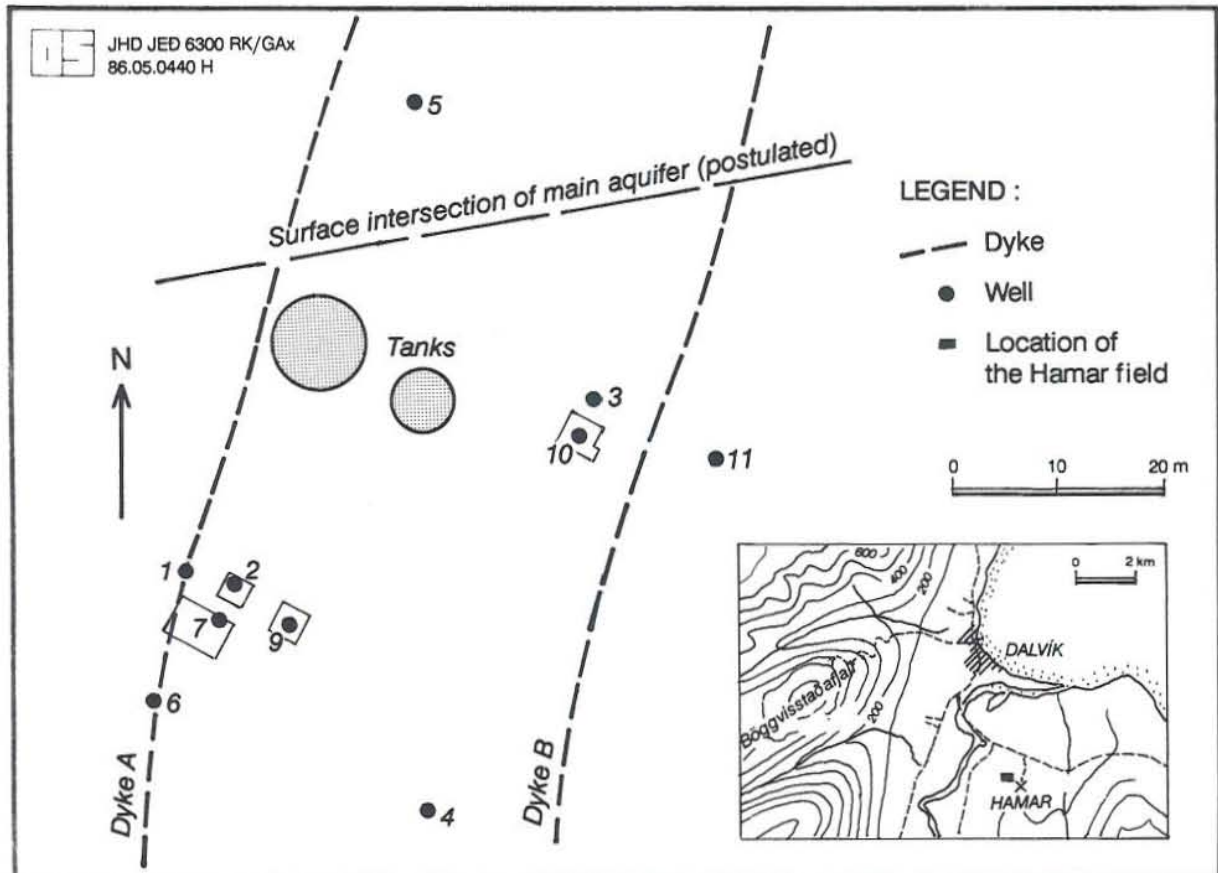

FIGURE 3: The Hamar geothermal field, location of wells (Karlsdottir et al., 1989)

3.1.2 Geology

The rock formations of the Hamar geothermal field mainly consist of Tertiary basaltic piles intercalated by layers of scoria and sediments. The field is intersected by two main dykes, (see Figure 3). Before any exploitation, there were some hot springs close to dyke A, but due to later production, they disappeared. At the start of utilization it was believed that flow would be controlled by dykes and, therefore, wells were located close to them.

3.1.3 Geophysics

The basic geophysical data was obtained from detailed ground magnetic measurements and head

on resistivity surveys. In the very beginning, the dykes were placed according to measured magnetic anomalies. Later on, by the use of the above mentioned head-on profiling, low resistivity areas, usually associated with high permeability zones, were found. These zones of relatively low resistivity were located in a westerly direction from the main dykes (Karlsdottir et al., 1989).

3.1.4 Production history

At the very beginning of production, the assumption was that the main aquifer was located in the thick layers of sandstones at a depth of around 100 to 180 m. Later, when drilling of well 10 was completed, another more permeable aquifer, at a depth from 700 to 800 m, was found. The main flow channel carrying hot water up to the surface is considered to be a vertical fracture, which is perpendicular to two above mentioned dykes. The well data is shown in Table 1.

TABLE 1:   Hamar field, well characteristics

Borehole no.	Date of completion	Depth (m)	Casing (m)	Depth of main aquifer (m)	In production
2	01 1969	300	38	186 - 226	1970-75
4	06 1969	303	28	205 - 215	no
5	02 1971	587	5	poor	no
6	03 1971	373	3	poor	no
7	07 1971	302	109	poor	no
9	09 1975	253	229	229 - 253	1975-77
10	09 1977	838	175	818	1977-88
11	08 1987	860	254	506 - 533	1988-.

The production data is shown in Table 2. More detailed data based on the average monthly production is shown in Figure 4. From these data, one can observe three specific periods of the production history. The first of them is characterized by the fast increase of production up to 1980 when the process of connecting the consumers was generally completed. The second period from 1980 to 1985 consists of five years of almost constant but high production and finally the third period, where a significant decrease of production can be observed. The explanation for this decrease in production is the fact that since 1986 the company changed its prior policy which resulted in less demand for hot water.

3.2   Calibration of aquifer parameters by the use of the AQUA program

3.2.1   Setting up the model

The total surface area covered by the mesh of nodes is about 200 km^2. Thus, the boundaries are taken far enough away to avoid their influence on the solution. The drawdown measurements from well 2 are used for calibration (see Figure 4).

As for the initial state, prior to production it was assumed that the reservoir water head was constant and the water level in each well depended upon its elevation above sea level, so that there was no hydraulic gradient in the area to begin with.

TABLE 2:   Hamar, average production of the field

Year	Production rate (l/s)	Wells in production
1970-73	22.5	2
1974	23.5	2
1975	29.1	2 and 9
1976	29.9	9
1977	30.6	9 and 10
1978	32.3	10
1979	37.2	10
1980	37.5	10
1981	39.9	10
1982	42.0	10
1983	41.1	10
1984	40.0	10
1985	40.8	10
1986	32.2	10
1987	26.4	10
1988	27.4	10 and 11
1989	26.4	11
1990	26.8	11
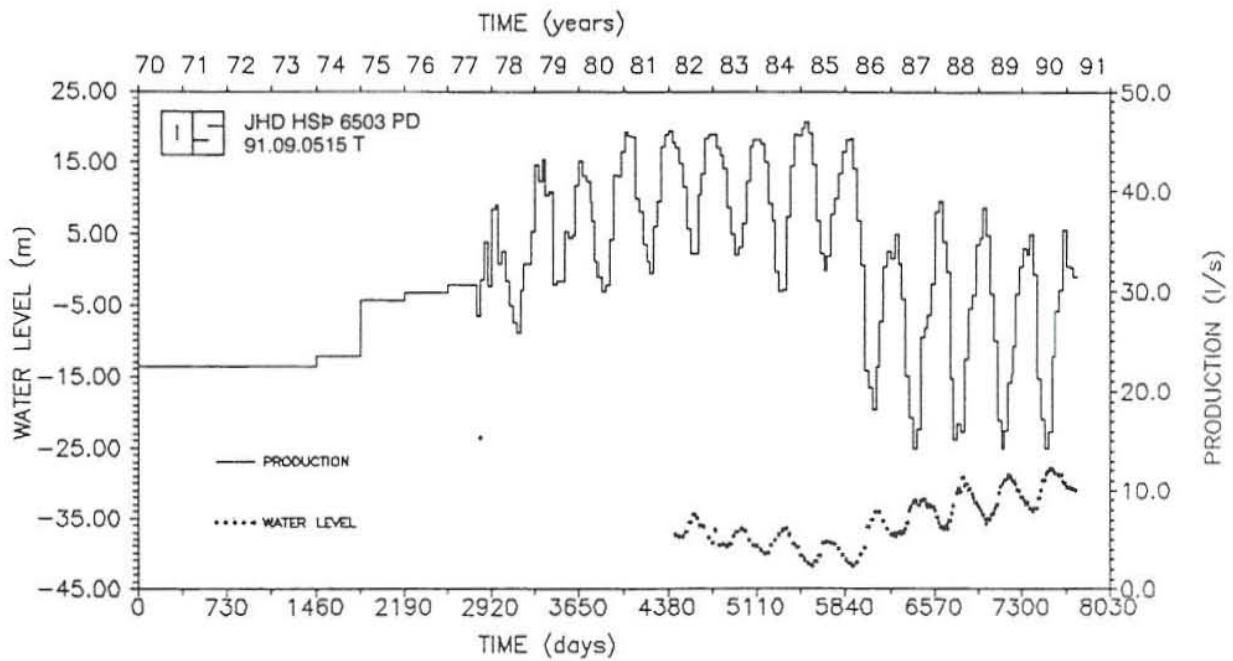
FIGURE 4:   The Hamar field, average monthly production

3.2.2 Flow problem

The main object of the calibration process in numerical modelling is to fit together calculated and measured time series of water level, concentration of dissolved minerals and temperature of geothermal water.

Taking the resistivity surveys and the geological features into account, the parameters in Equation 33 were fitted to give the best match between observed and calculated values. The result is as follows:

transmissivity   *from 1.5 x 10^{-5} to 1.35 x 10^{-2} m^2/s* (Figure 5),
storage coefficient   *1.3 x 10 $^{-3}$,*
leakage coefficient   *2.0 x 10 $^{-10}$,*
porosity   *20%,*
thickness of aquifer   *650 m,*
delay constant   *100 days.*

.1350 E-01 m^2/s
.2550 E-02 m^2/s
.1350 E-02 m^2/s
.1500 E-04 m^2/s
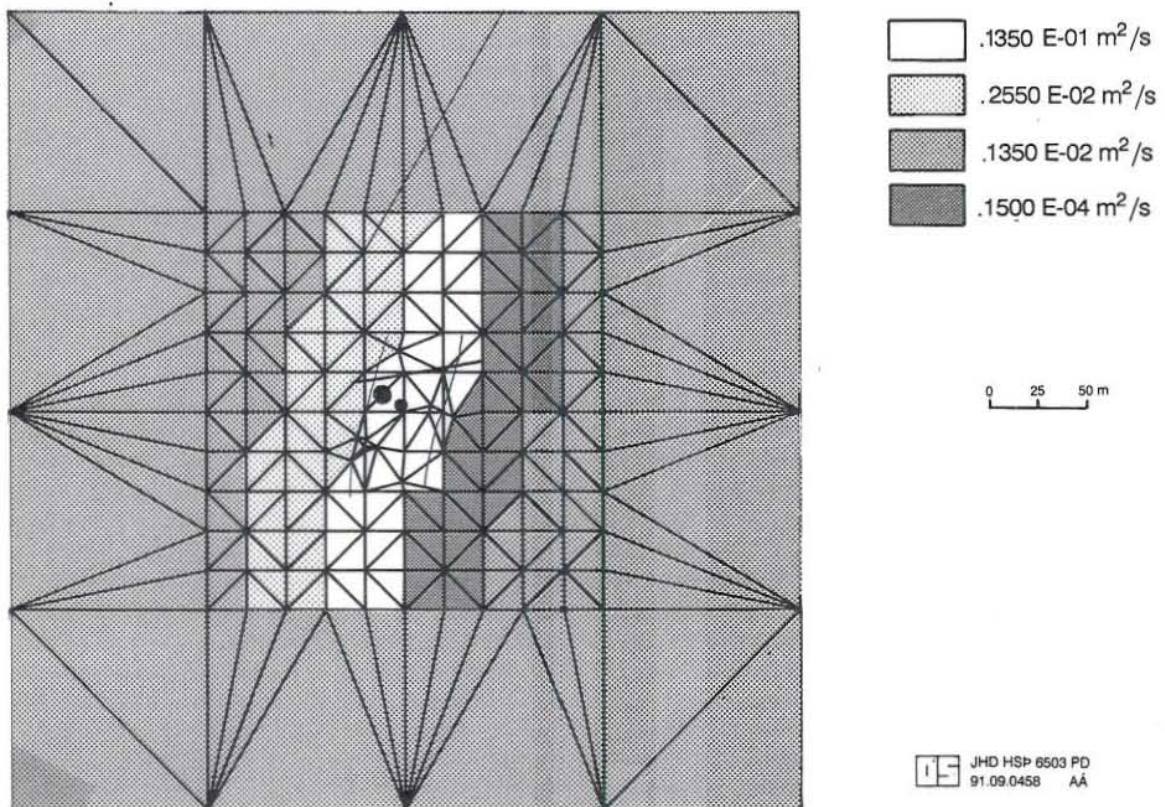
FIGURE 5: The Hamar field, map of transmissivity

Figure 6 shows calculated and measured drawdown for the Hamar field. The map of calculated drawdown is in Figure 7.

3.2.3 Mass transport

Mass transport calculation can be used to estimate leakage coefficient and aquifer thickness. By fitting the calculated and measured values of silica concentration, the above mentioned parameters can be calculated (see Figure 8).
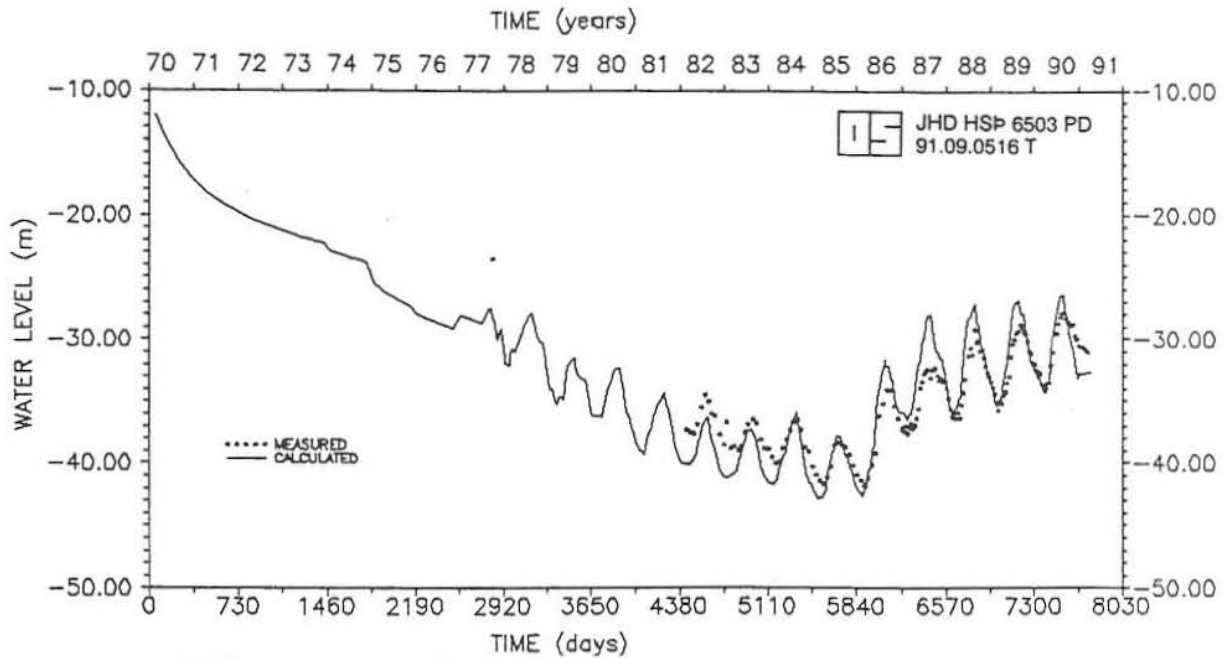

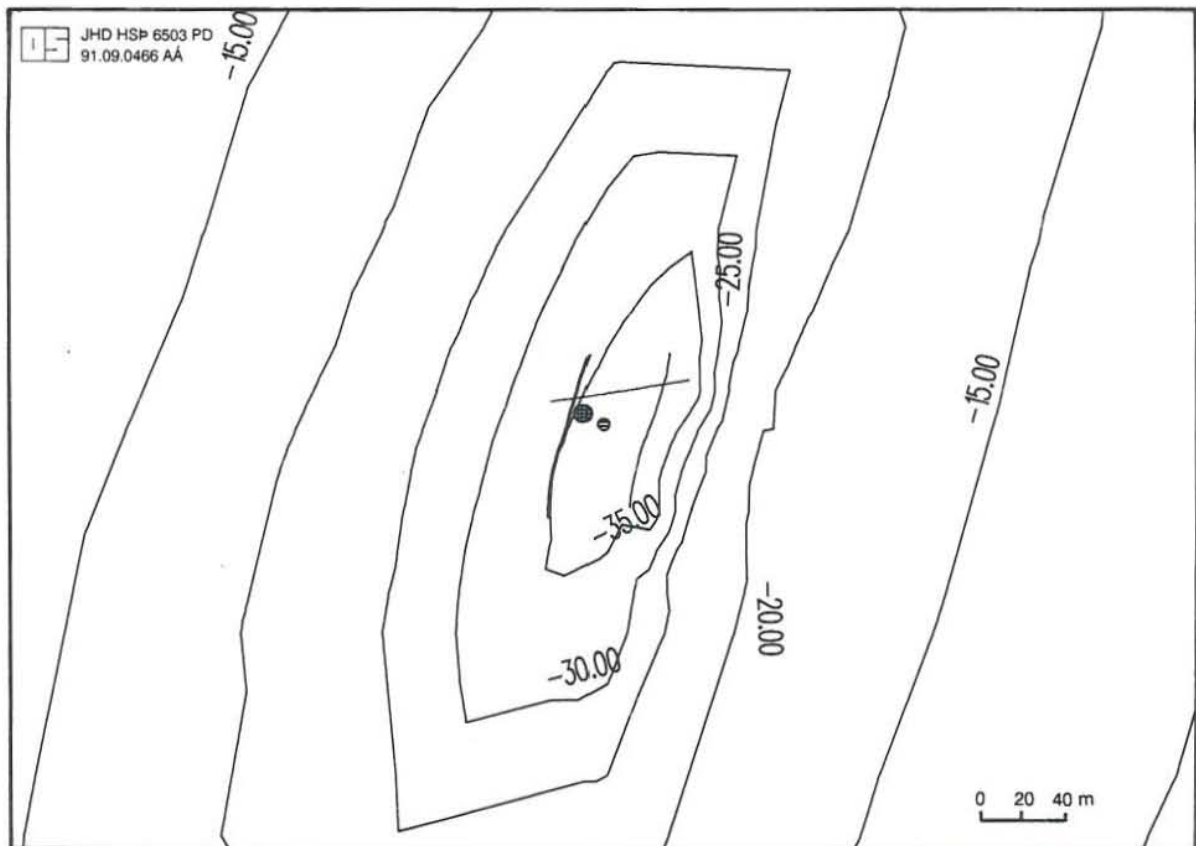FIGURE 6: The Hamar field, calculated and measured drawdown

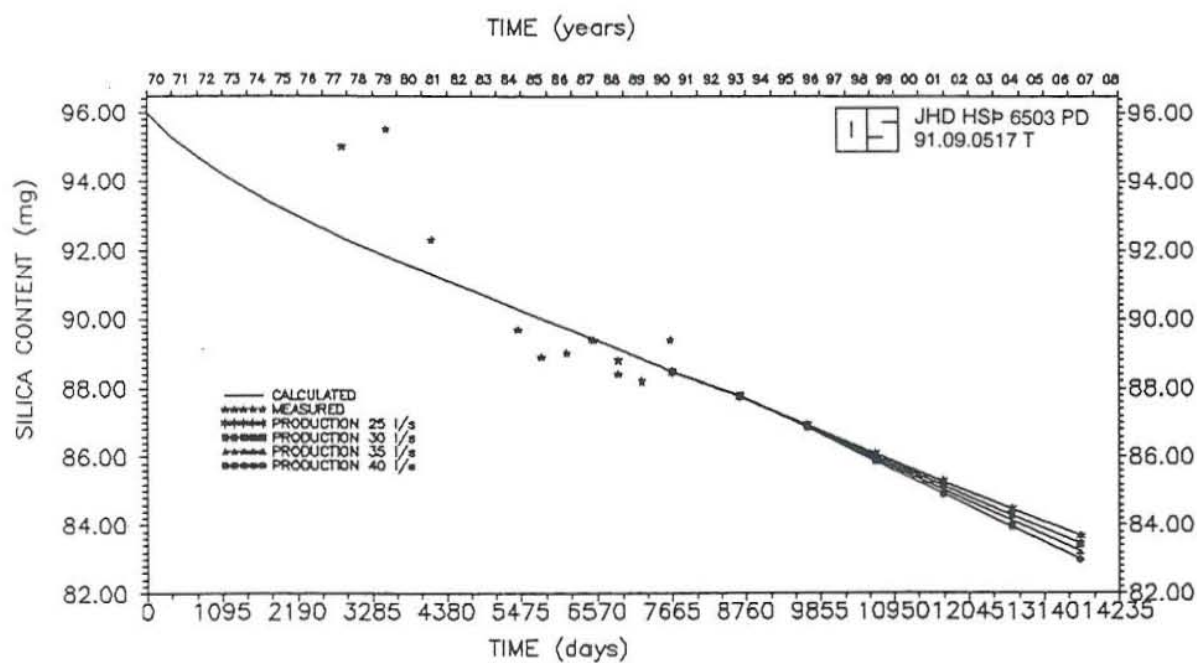FIGURE 7: Hamar field, map of calculated drawdown (m), in 1991

TIME (years)

FIGURE 8: Mass transport and prediction of silica content until year 2006

3.2.4 Heat transport

Considering the almost constant temperature of 64°C of pumped water from the reservoir, heat transport calculation can be used to test the appropriate choice of aquifer thickness and porosity. Results of calculations are shown in Figure 9 and confirm that there have been no significant changes in reservoir temperature during the 20 years of exploitation.
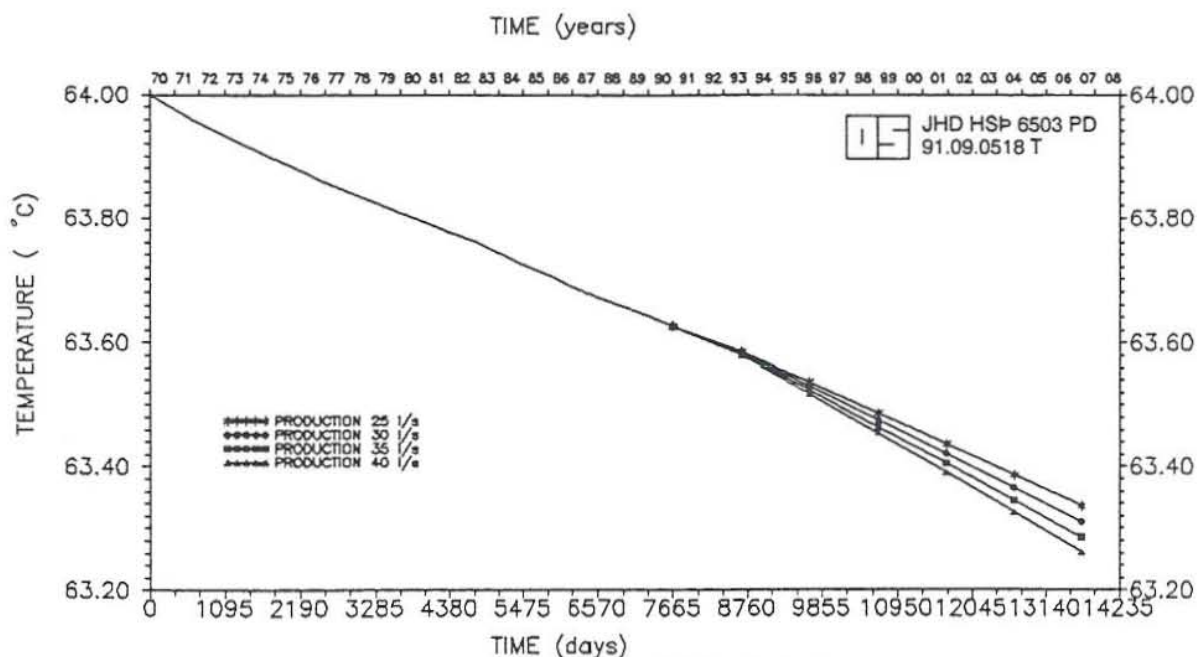
TIME (years)

FIGURE 9: Prediction of reservoir temperature until year 2006

3.2.5 Future predictions

In fact, future prediction of reservoir behaviour is the main object of all calibration efforts. Based on the final, best fitted model, three forecasts until the year 2006, concerning water level, concentration of silica and reservoir temperature are made, respectively.
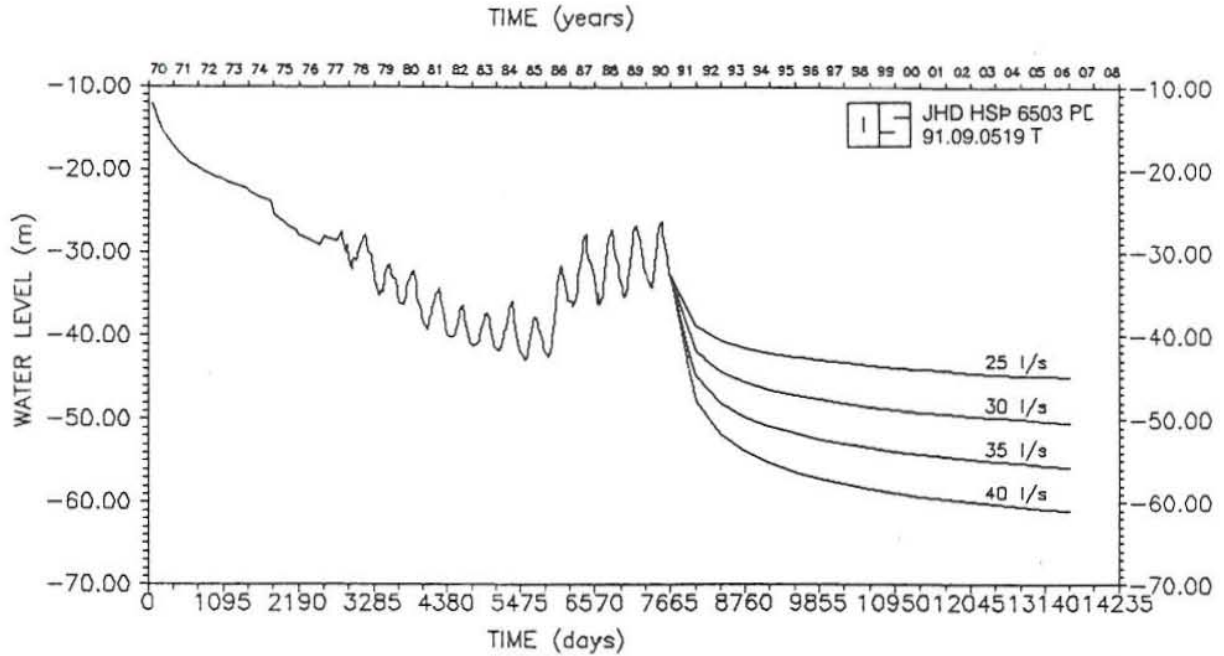

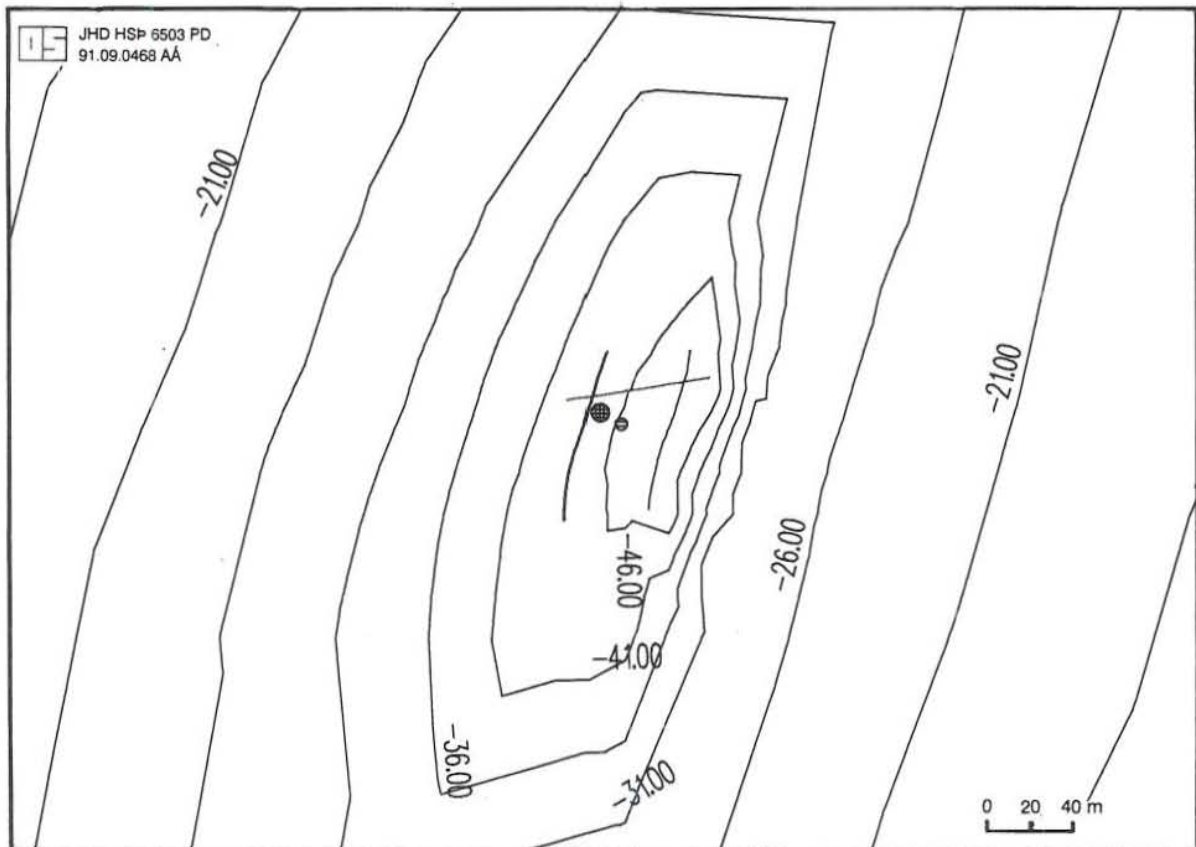FIGURE 10: Prediction of water level with different pumping rates until the year 2006

FIGURE 11: Map of calculated drawdown (m) in the year 2006 for a production of 25 l/s

As a starting point for future predictions, the reservoir state from 1991 is taken. The calculations are made with four different production rates: 25, 30, 35 and 40 l/s. All calculated curves of future water levels in Figure 10 show a lowering trend. The obtained drawdowns are between 45 m for a production of 25 l/s and 61 m for a production of 40 l/s. Results mentioned above are average values and do not take into account the seasonal changes in production. In addition, Figures 11 and 12 show the areal distribution of drawdown in the year 2006, for the production rates of 25 l/s and 40 l/s, respectively. In addition to the calibration period, future predictions concerning the reservoir temperature and the concentration of silica are presented in Figures 8 and 9. In the case of temperature, no significant cooling can be observed, even for the largest production rate.
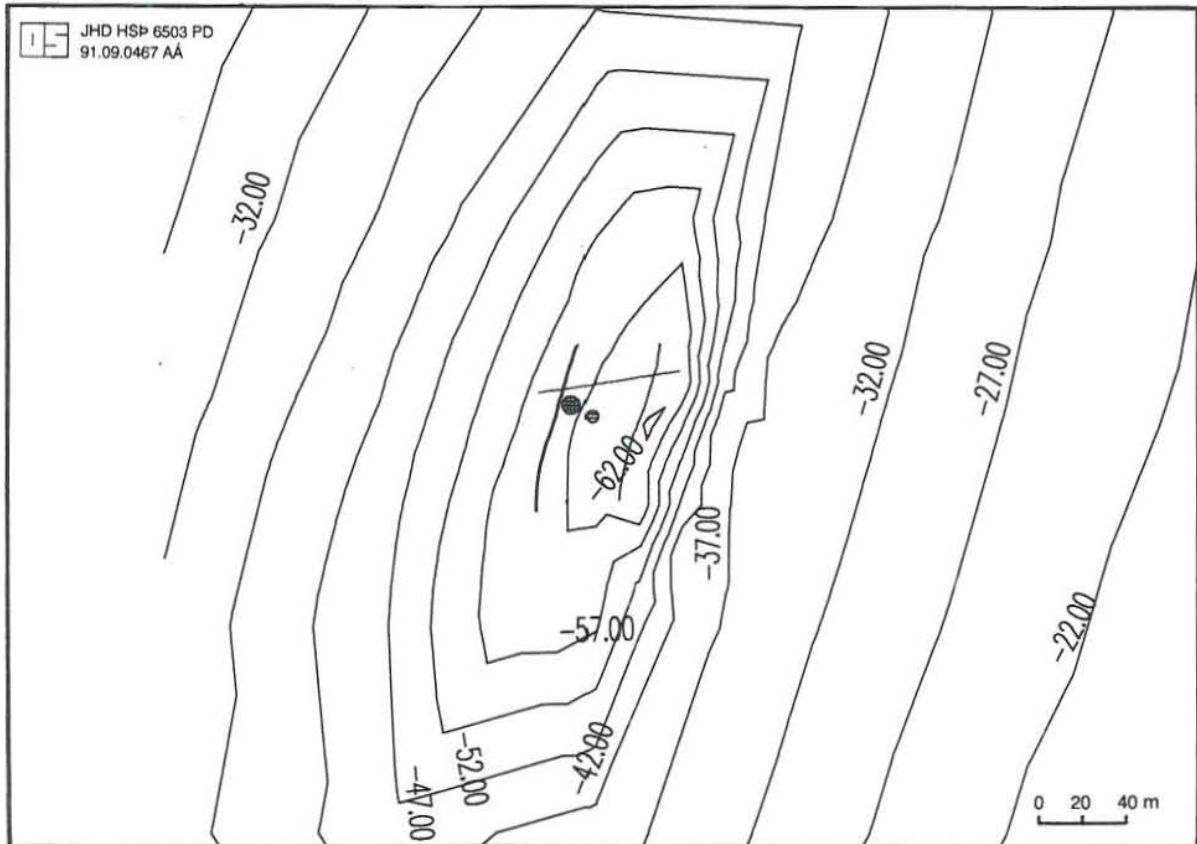

FIGURE 12:   Map of calculated drawdown (m) in the year 2006 for a production of 40 l/s

4. MODELLING OF THE PODHALE GEOTHERMAL FIELD, S-POLAND

4.1 The main features of the Podhale geothermal field

4.1.1 Locality

The Podhale field is located in S - Poland, on the border of Czechoslovakia, about 100 km south of the city of Cracow. The total area of the Podhale field is about 1000 km^2 and about 500 km^2 lie within polish frontiers; the rest of the field belongs to Czechoslovakia. This is the most famous and important tourist and winter sport region of the country, and where Zakopane, the largest ski resort, is situated (Figure 13).

FIGURE 13: Podhale geothermal field, map of location

4.1.2 Geology

Podhale geothermal field is a type of a sedimentary basin. This basin is located between the Tatra Mountains in the south and Pieniny Clippen Belt in the north. These two geological structures form natural boundaries of the geothermal reservoir. The basin is a kind of asymmetric syncline, with the longer, main axis E-W, and shorter N-S. The N-S geological cross-section through the basin can be characterized as follows: the cap rock is of Tertiary age and is built of sandstone layers intercalated by shales. The thickness of this formation reaches 2500 m in the central part of the basin. The main aquifer is situated at a depth, from 1000 m in the vicinity of Tatra Mountains up to 2500 m in the central part of the syncline. The thickness varies from tens to several hundreds of meters. The reservoir is constituted of limestones and dolomites of Eocene and Mesozoic age. Further aquifers could occur to a depth of 5000 m, probably under the main reservoir.

The geothermal resources are of low enthalpy type. The temperature of the geothermal water is in the range of 95°C in the deepest part of the basin to about 60°C in the vicinity of the outcrops of the aquifer. These outcrops occur on the northern slopes of Tatra Mountains, where the recharge area is probably also located. The total mineralization of the geothermal liquid does not exceed 3 g/l, and is in the most favourable conditions about 0.5 g/l.

4.1.3 Geophysics

Several seismic profiles cross the Podhale basin, both in E-W and N-S directions. A seismic survey was carried out due to oil and gas exploration, and some regional magnetic and gravimetric measurements also took place in this area. Very detailed interpretation of seismic profiles was difficult because of very complicated fault tectonics. Nevertheless, the general assumptions based on these measurements were confirmed by the results of drilling works.

4.1.4 State of development

At the present time, seven deep boreholes have been drilled within the geothermal field. All of them are good producers of hot water. In six wells the artesian well head pressure is in the range from 15 to 28 bars and the free flow from each well is 60 l/s. The main reason for developing the geothermal resources is the demand for energy for space heating, so hot water could be supplied substituting the coal firing, which is common in the region. It is worthwhile to mention that the main components of air pollution in Podhale region are born in the firing of coal.

The technology of heat supply is based on the utilization of two wells for one plant, one for production and a second for reinjection (in France it is called "geothermal doublet"). As was mentioned above, without using any pumps, the aquifer can supply about 60 l/s of water at a temperature of 86°C. Heat is extracted at the surface and afterwards the cooled water is reinjected at a temperature about 30°C or less into the same aquifer. This technology is obviously more expensive than throwing away the waste water, but is environmentally harmless as well as preventive of pressure decline during long term production. Besides the space heating, geothermal water will be supplied to heat greenhouses and swimming pools. The main economic advantages of geothermal heating in this part of Poland, is the long heating season, which lasts about 300 days per year.

4.2 Simulation of reservoir behaviour by the use of the AQUA program

4.2.1 Setting up the model

The main reason for carrying out the simulation of the geothermal doublet behaviour, is the need to obtain information about its life time and breakthrough time. As a first step the distributed model of the whole reservoir was established on the basis of all available geological and hydrological data. According to data from wells as well as seismic profiles, the different values of transmissivity were used (Figure 14).
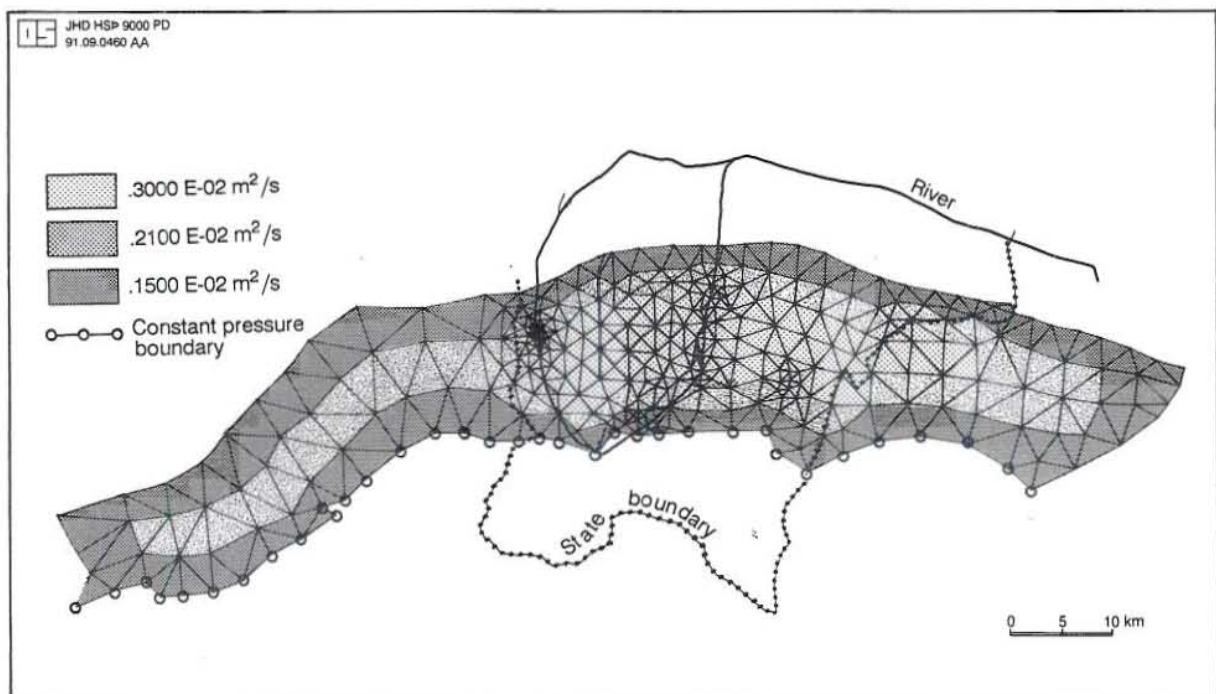

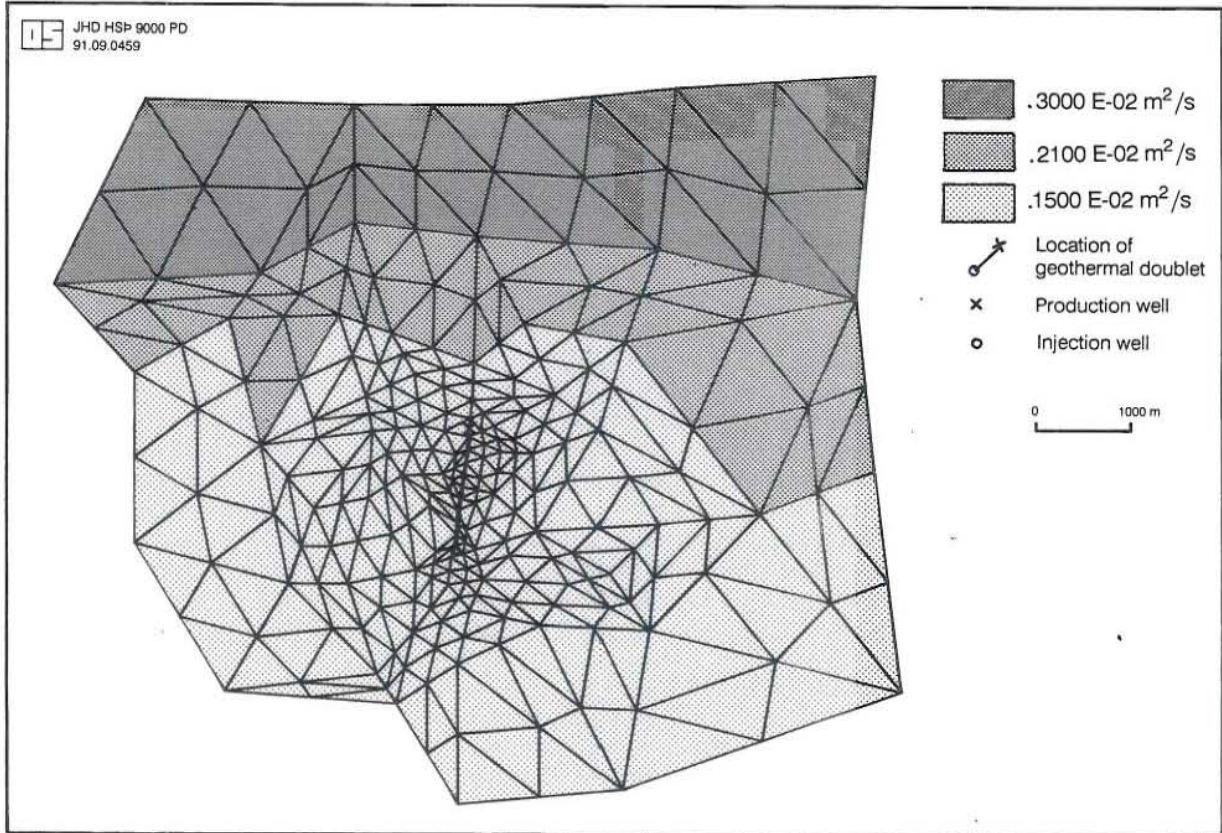FIGURE 14: Podhale field, map of transmissivity

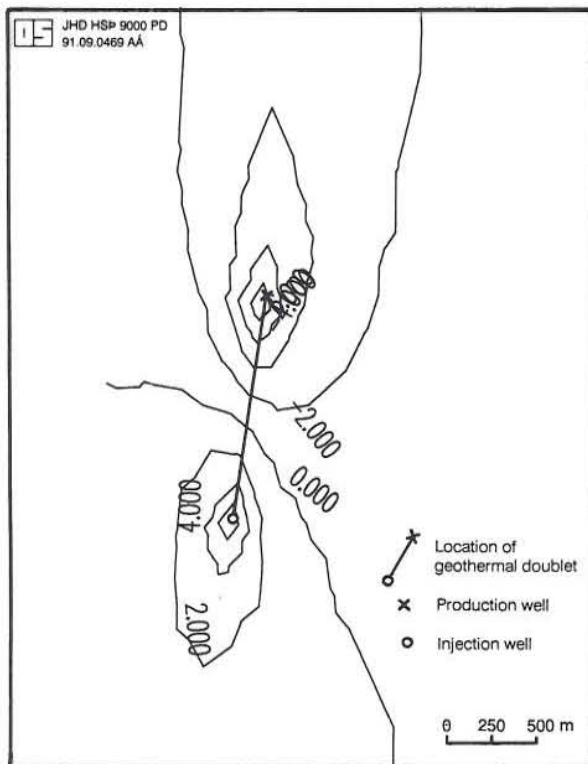Figure 15: Podhale field, map of transmissivity in the vicinity of the geothermal doublet

FIGURE 16: Calculated drawdown (m),
for a production of 20 l/s

The lowest value of transmissivity covers most of the external part of the basin and gradually increases towards the central part. These changes are related to the increase in aquifer thickness from the outcrops to the main axis of a syncline. It is believed that the southern boundary of the
field, where outcrops are located, is the main recharge area as well. Therefore, taking that into account, the southern boundary is established as a boundary with constant head conditions. The rest of the boundaries act as no-flow boundaries, according to geological structures forming the reservoir. Anisotropy, which is determined by anisotropy angle and by the ratio between T_{xx} and T_{yy}, is established on the basis of the main fault's direction within the field; the parameters have values 90° and 10° respectively. Figure 15 shows the distribution of transmissivity in the vicinity of the geothermal doublet.

4.2.2 Flow problem

Three possibilities of different pumping and reinjection rates are considered. In this case the stationary flow problem was solved, with the assumptions that neither leakage nor infiltration occur. For the production-injection rate equal to 20 l/s, the extreme values of water head are respectively -8.2 m and 6.2 m (Figures 16 and 17).
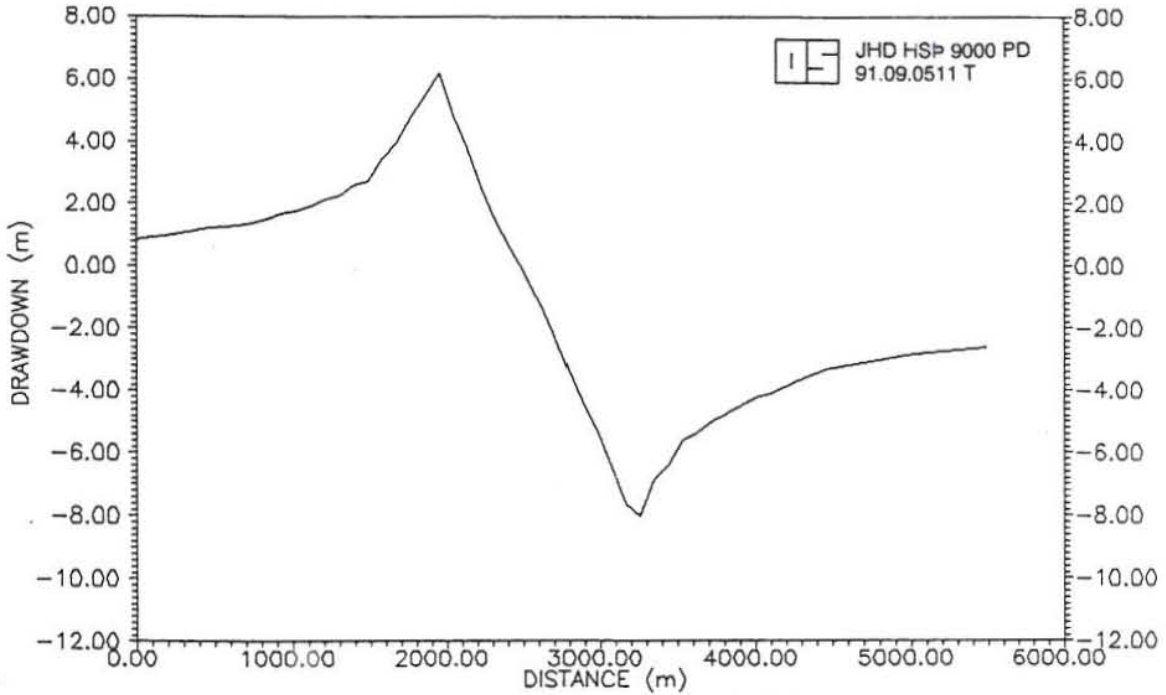

FIGURE 17: Cross-section of drawdown (m), for a production of 20 l/s

Values of drawdown in the case of production-injection rate equal 50 l/s are shown in Figures 18 and 19.
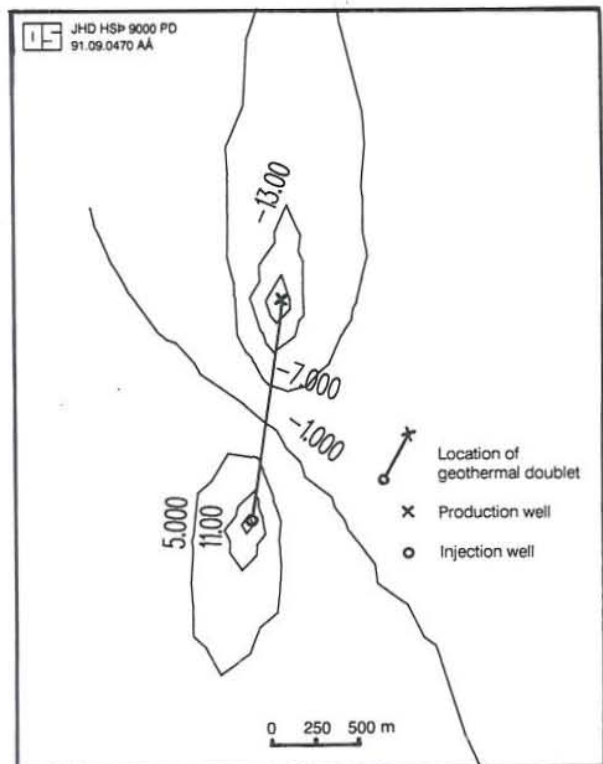
FIGURE 18: Calculated drawdown (m), production 50 l/s
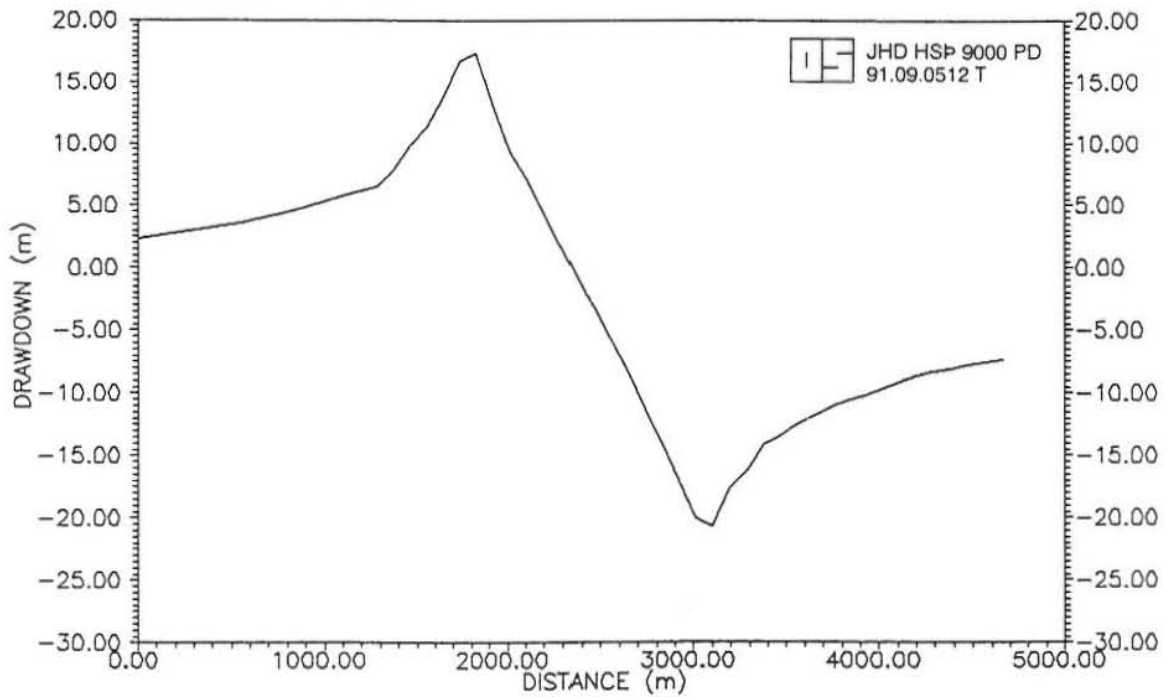
FIGURE 19:   Cross-section of drawdown (m), for a production of 50 l/s

As the last case, 100 l/s of production and injection were considered, yielding the lowest /value of drawdown in the production well, -45 m, and the highest increase of pressure in the injection well, 37 m (Figures 20 and 21).
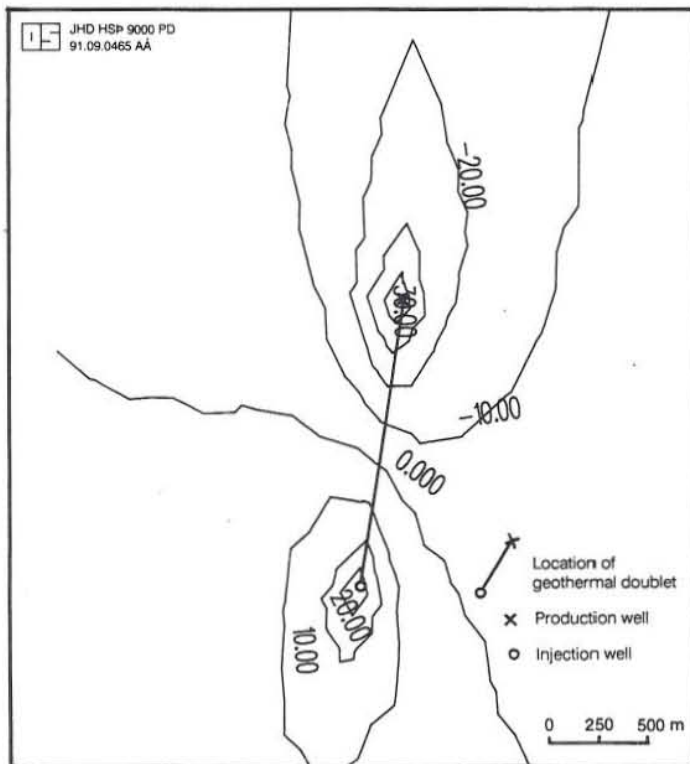

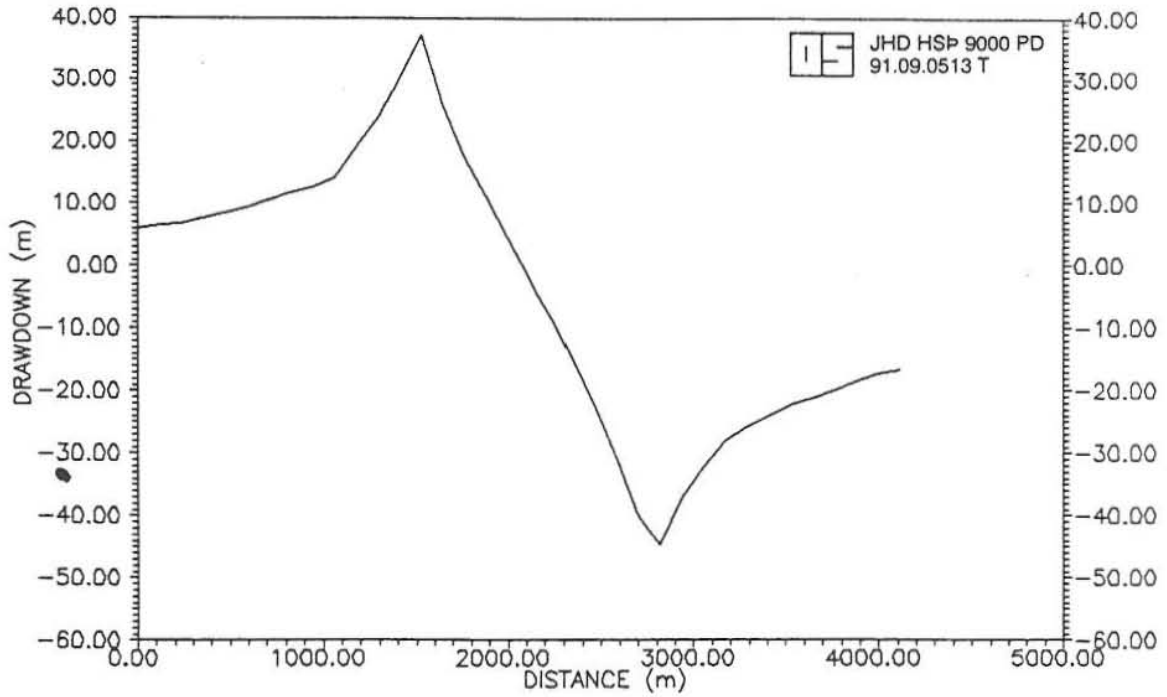FIGURE 20:   Calculated drawdown (m), for a production of 100 l/s

FIGURE 21: Cross-section of drawdown, for a production of 100 l/s

Figure 22 presents the flow intensity within the geothermal doublet; the size of arrows is related to the amount of displaced liquid.
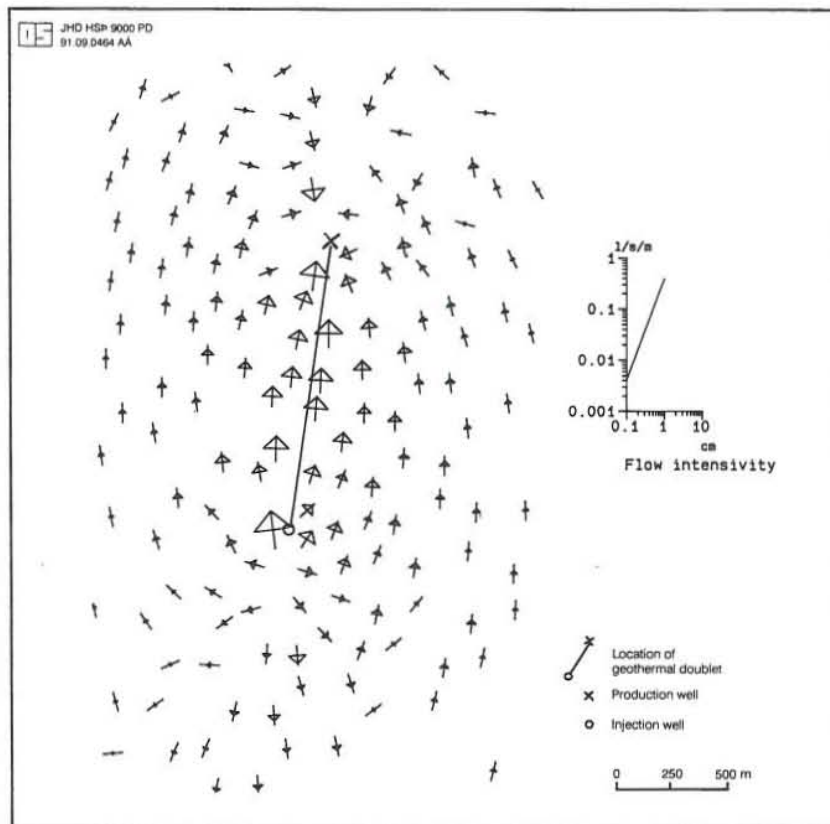

FIGURE 22: Map of flow paths within geothermal doublet, for a production of 100 l/s

4.2.3 Heat transport

The injection-production process induces an artificial velocity field and a hydraulic connection between the wells. After a specific period (breakthrough time), an increasing amount of the injected water reaches the production well. This specific time is a function of reservoir parameters, geometry and production-injection rate. A second important feature of the geothermal doublet appears when the cold waters reach the production well at thermal breakthrough time and start to decrease the production temperature. This phenomena controls the life time of the geothermal plant (Menjoz A., 1990).

As in a previous subchapter, three values of production-injection rates are considered. The initial temperature of the production well is 86°C and after extraction of heat, it is cooled down to 30°C before it is injected back into the reservoir. Parameters used in solving the transient transport problem, by which the breakthrough and life time were calculated, are as follows:

porosity of reservoir	*10%*
longitudinal dispersivity	*100 m*
retardation constant	*0.226*
aquifer thickness	*500 m*

Results of simulations are shown in Figures 23, 24, 25, 26.

For the production-injection rate of 20 l/s, the first change in temperature of the produced liquid, recognizing 0.5°C as such change in temperature, can be observed after 130 years of production. For 50 l/s, breakthrough time, as defined above, will take place after 40 years and finally for production - injection rate 100 l/s it will be after 26 years.

In the same way, one can estimate the practical life time of a geothermal doublet, for a prescribed temperature drop of 3°C. These periods for the same rates of production - injection are respectively 220, 84 and 44 years of exploitation.
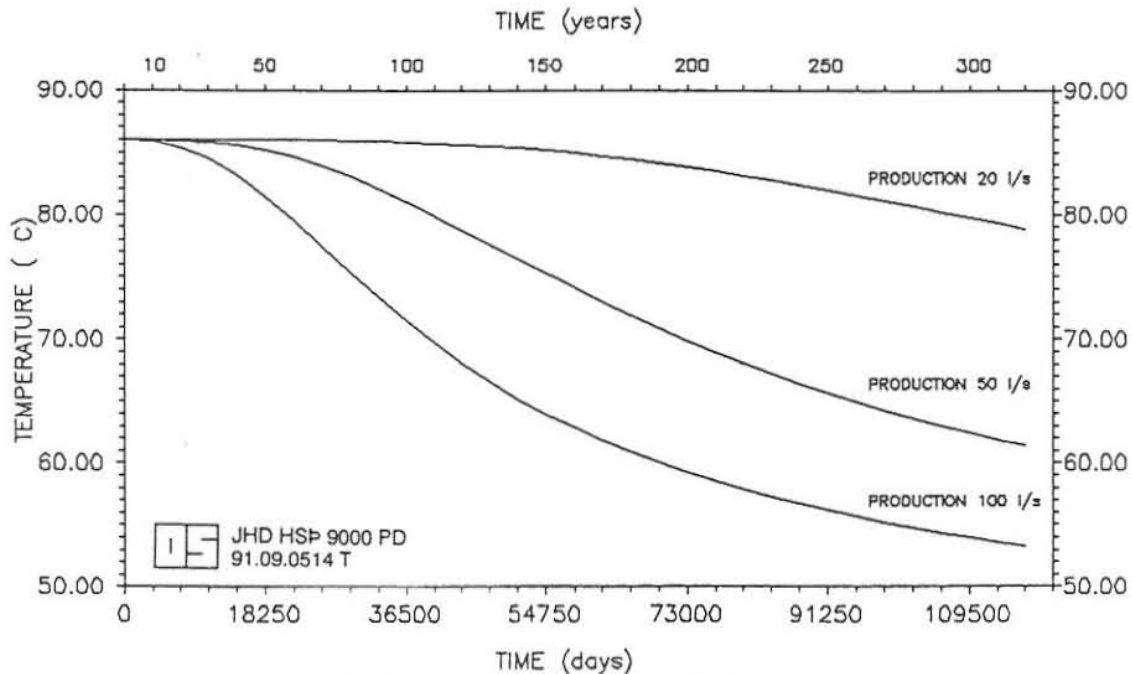

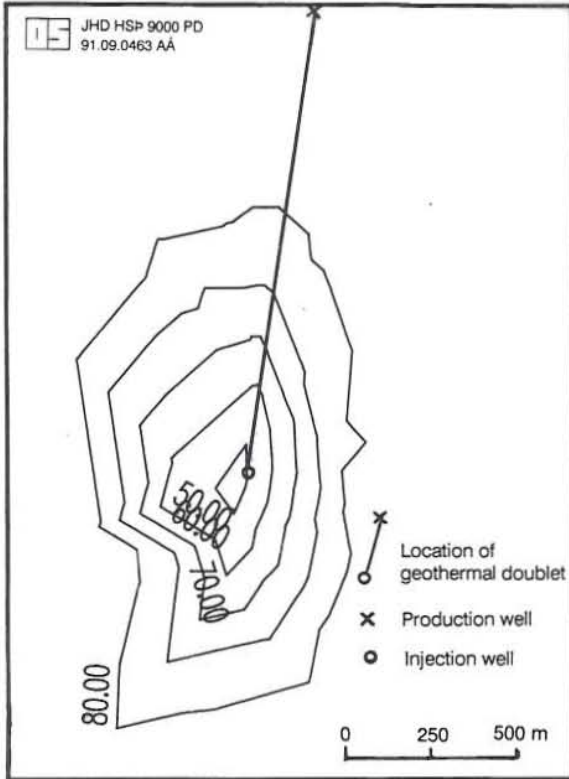FIGURE 23: Calculations of breakthrough time for a geothermal doublet with different production rates

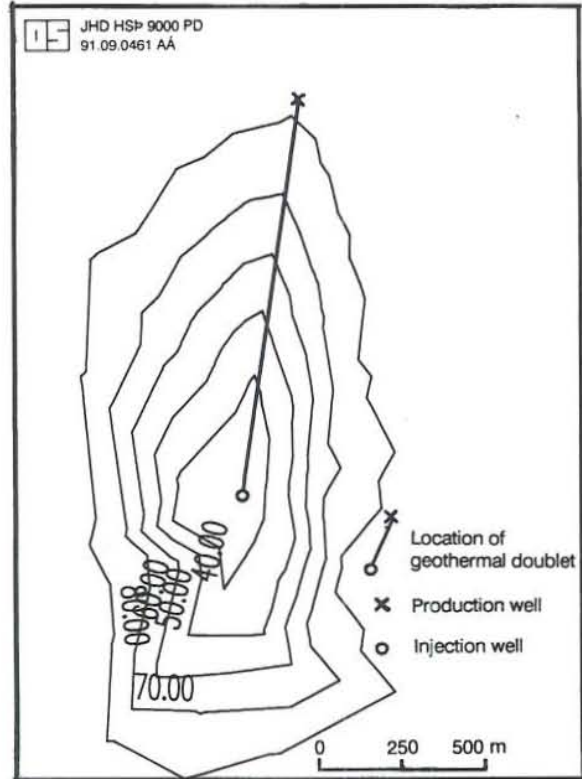FIGURE 24: Distribution of temperature (°C) after 100 years, production 20 l/s

FIGURE 25: Distribution of temperature (°C) after 100 years, production 50 l/s

The theoretical breakthrough time can be compared with the AQUA solution by finding the time it takes the temperature of the pumped well to reach the average temperature of the injection well and the initial reservoir temperature, which is equal to (86°C + 30°C)/2 = 58°C.

The formula, based on a sharp front model, can be expressed as

$$t_{breakthrough} = \frac{4\pi b\kappa\varphi x_0^2}{3Q} \qquad (42)$$

where

$$\kappa = 1 + \frac{(1-\varphi)\rho_s c_s}{\varphi \rho_w c_w} \qquad (43)$$

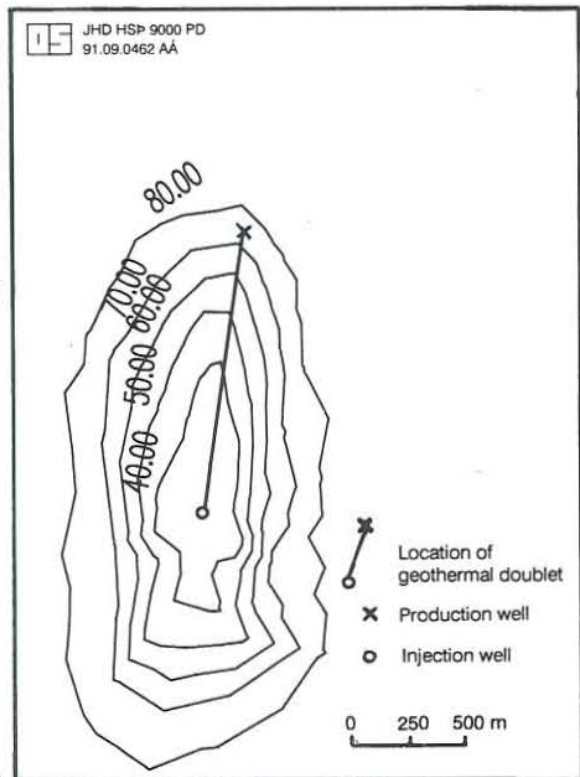Values of the parameters used in these calculations are shown in Table 3.

FIGURE 26: Distribution of temperature (°C) after 100 years, production 100 l/s

TABLE 3:   Values of parameters used in sharp front model

Symbol	Name of parameter	Value
b	thickness of aquifer	500 m
φ	porosity of aquifer	10%
x_0	half distance between boreholes	620 m
Q_1	production rate	20 l/s
Q_2	production rate	50 l/s
Q_3	production rate	100 l/s
ρ_s	density of the porous medium	2500 kg/m^3
ρ_l	density of the water	1000 kg/m^3
c_s	specific heat capacity of the porous medium	1000 kJ/kg°C
c_l	specific heat capacity of the water	4200 kJ/kg°C

Results of the calculations are in Table 4.

TABLE 4:   Comparison of breakthrough time calculations
for sharp front and distributed parameter models

Production rate (l/s)	Sharp front model $t_{breakthrough}$ (years)	Distributed parameters model $t_{breakthrough}$ (years)
20	810	1000
50	324	400
100	162	215

The differences in the obtained results can be explained by the absence of dispersivity in the calculations based on the sharp front model.

5. CONCLUSIONS

Further production from the Hamar geothermal field should not be faced with any serious problems within the next 15 years. In reference to results obtained in the calibration process and for future predictions, the constant lowering of the water level is observed but with a tendency towards a semi-steady state if the production rate does not exceed 40 l/s. One has to remember that calculations assume constant production rate throughout the year. In the case of the largest pumping rate of 40 l/s, one can expect the drawdown in the year 2006 to be approximately 62 m. Future predictions of reservoir temperature indicate almost no changes within the next 15 years. For the 40 l/s production rate, the calculated decrease of temperature in the year 2006 is about 0.7°C.

Results obtained in the simulation of a geothermal doublet allow us to design a heating system, which will be able to work during the next 45 years, supplying about 100 l/s of water with a temperature of 86°C to 83°C. Calculations of expected changes in wellhead pressure of production and injection wells indicate that the size and capacity of pumps, which should be used in maintaining the doublet work, are typical and widely available.

REFERENCES

Bodvarsson, G.S., and Witherspoon, P.A., 1989: Geothermal reservoir engineering. Part I. Geothermal Science and Technology, 2-1, 1-68.

Boulton, N.S., 1963: Analysis of data from non-equilibrium pumping tests allowing for delayed yield from storage, Proc. Insin. civ. Engrs. (London), 26, 469-482.

Karlsdottir, R., Eysteinsson, H., Smarason, O.B., Axelsson, G., and Sigurdsson, O, 1989: The drilling of well 11 at Hamar in Svarfadardalur. Orkustofnun, Reykjavik, report OS-89049/JHD-22 B (in Icelandic), Reykjavik, 44 pp.

McWhorter, D.B, and Sunada, D.K., 1977: Ground water hydrology and hydraulics. Water Resources Publications, Fort Collins, Colordo, 290 pp.

Menjoz, A., 1990: Lectures on the characterization and exploitation of geothermal reservoirs in France. UNU G.T.P., Iceland, report 2, 89 pp.

Vatnaskil Consulting Engineers, 1990: AQUA user's manual. Vatnaskil, Reykjavik.